

Anodic Stripping Determination of Selenium in Seawater Using an Electrode Modified with Gold Nanodendrites/Perforated Reduced Graphene Oxide

Hong Wei^{1,2}, Dawei Pan^{1,2,*}, Yuanding Cui³, Haiying Liu³, Guangheng Gao⁴, Jianjun Xia^{5,*}

¹ Key Laboratory of Coastal Environmental Processes and Ecological Remediation, Yantai Institute of Coastal Zone Research, Chinese Academy of Sciences, Yantai 264003, P.R. China.

² University of Chinese Academy of Sciences, Beijing 100049, P.R. China

³ Electromechanical Engineering Institute, Jiangxi Application Engineering Vocational College, Pingxiang 337042, P.R. China

⁴ Biology Institute, Qilu University of Technology (Shandong Academy of Sciences), Key Laboratory for Biosensors of Shandong Province, Jinan 250353, P.R. China

⁵ Research and Development of Center, China Tobacco Yunnan Industrial Co., Ltd., Kunming 650231, P.R. China.

*E-mail: dwpan@yic.ac.cn , lordxia@126.com

Received: 24 October 2019 / Accepted: 4 December 2019 / Published: 31 December 2019

Anodic stripping voltammetric determination of selenium was successfully and effectively performed using an electrode modified with gold nanodendrites/perforated reduced graphene oxide (AuNDs/P-rGO), which was synthesized via a facile electrochemical deposition route. The compositions of the AuNDs/P-rGO were characterized by Scanning electron microscopy. The experimental parameters of the Se(IV) accumulation, Se(IV) potential, the gold deposition time and the interference by other ions were discussed in detail. The linear range of selenium at the AuNDs/P-rGO modified electrode was from 3 nM to 300 nM, with a detection limit of 0.9 nM under optimized conditions. The proposed electrode showed satisfactory results in both real seawater samples and standard artificial seawater samples with different salinities.

Keywords: Electrochemical deposition; square wave voltammetry; Se(IV); seawater; spiked seawater sample

1. INTRODUCTION

Selenium (Se) is a micronutrient that is essential for the growth and development of humans and animals [1-3]. The metabolism of Se in the human body typically occurs via the route: Se(IV) → H₂Se → DMSe (dimethyl selenide) → DMSe⁺ → respiration via the respiratory tract or urethra. In particular,

the chemical form of and concentration of selenium affect its biological properties in the human body. Se(IV) and Se(VI) are the most common oxidation states of Se, and Se(IV) is more toxic than Se(VI) [4]. The total Se concentration in seawater is typically less than 200 ng/L [5] but in some areas, it can reach 400 µg/L [6,7]. Se(IV) poses a series of hazards to the human body once its concentration exceeds a certain threshold value, including certain threats to cells and tissues which cause irreversible damage [8]. Moreover, dissolved metals in seawater have a higher bioavailability and mobility, and they can easily harm marine ecosystems and organisms. Therefore, from the perspective of marine management, ecological security, and human health, it is necessary and urgent to establish a reliable analytical method to accurately detect Se(IV) in marine environments. Over the last few years, research has been conducted to determine selenium in water environments, including electrothermal atomic absorption spectroscopy (ET-AAS) [8], gas chromatography (GC) [9], hydride generation atmospheric pressure glow discharge optical emission spectrometry (HG-APGD-OES) [10], inductively coupled plasma-mass spectrometry (ICP-MS) [11,12], microwave plasma atomic emission spectrometry (MP-AES) [13], and mass spectrometric analysis [14]. However, those methods are considerably low cost-effective, and require complex pre-treatment, especially for high-salt matrix water sample. Comparatively, electrochemical detection methods [15,16] have certain technical advantages when used to detect heavy metals in seawater, including a fast analysis speed, high sensitivity, simple pre-treatment process, and small influence by the high salt content of seawater [17-19]. Since the +IV oxidation state of Se is the only electroactive species, electroanalytical techniques may be alternatives for Se(IV) determination [20]. Thus, electroanalytical detection appears promising for determining Se(IV) in seawater samples with high salinities. Extensive research efforts have been devoted to developing suitable electrodes for the determination of Se(IV) using electrochemical methods, including copper-modified mercury-film electrodes [21], bismuth film electrodes [22], renewable silver annular band working electrodes [23], screen printed graphite electrodes [24], and gold nanoparticle modified glass carbon electrodes (AuNPs/GCE) [25]. However, the vast majority of the methods for detecting water samples are primarily for lower-salinity water (e.g., drinking water and river water). As for the seawater, a higher salinity is one of the most difficult issues to overcome for the accurate determination of Se(IV) [26].

Gold nanomaterials have excellent conductivity and tunable sizes and have been successfully used as electrode materials in electrochemical applications [27-29]. Graphene has been widely used because of its high thermal conductivity, large specific surface area, and unique catalytic properties [30]. Prussian blue (PB) can be arbitrarily design the presence, especially in alkaline solutions [31-33], therefore, it was used as a green flexible template to synthesize porous graphene in this experiment. Based on our previous report [34], a gold nanodendrites/perforated reduced graphene oxides (AuNDs/P-rGO)-modified electrode was constructed by combining dendritic gold nanoparticles using high-performance perforated reduced graphene oxide as the electrode substrate.

Herein, the application of an AuNDs/P-rGO-modified electrode was further investigated to detect Se(IV) in different saltwater samples. Furthermore, the experimental parameters of the Se(IV) accumulation, Se(IV) potential, and the gold deposition time were also discussed in detail. As far as the authors know, no reports have been published for Se(IV) determination using GC/AuNDs/P-rGO so far. Additionally, the preservation and storage of seawater samples was also examined. Moreover, the

application of GC/AuNDs/P-rGO to determine Se(IV) in real seawater and standard artificial seawater samples with different salinities showed a good response and satisfactory results.

2. EXPERIMENTAL SECTION

2.1. Reagents

Standard stock solutions of Se^{4+} , Fe^{3+} , Co^{2+} , Pb^{2+} , Sb^{3+} , Cu^{2+} , Mg^{2+} , and perchloric acid (HClO_4) were purchased from Acros Organics. Graphene oxide (GO) was obtained from Nanjing XFNANO Materials Tech Co., Ltd. (Nanjing, China). Chlorauric acid (HAuCl_4), potassium ferricyanide ($\text{K}_3\text{Fe}(\text{CN})_6$), ferrous sulfate (FeSO_4), sulfuric acid (H_2SO_4), nitric acid (HNO_3), sodium hydroxide (NaOH), and hydrogen peroxide (H_2O_2) were supplied by Sinopharm Chemical Reagent (Shanghai, China). All other chemicals were analytical-grade and were no further purified. Deionized water (18.2 $\text{M}\Omega$ cm specific resistance) was prepared using a Pall Cascada laboratory water system and used throughout the experiments.

2.2. Apparatus

Electrochemical experiments, including cyclic voltammetry (CV) and square wave voltammetry (SWV) were performed on a CHI 660E electrochemical workstation (ChenHua, Shanghai, China). The modified GC (3 mm in diameter) was used as the working electrode, with an Ag/AgCl electrode and platinum foil serving as the reference and counter electrodes, respectively. The morphology of AuNDs/P-rGO-modified electrode were recorded on scanning electron microscopy (SEM, Hitachi S-4800 microscope, Japan). ICP-MS (ELAN DRC, Perkin Elmer Instruments) was used for comparative testing of selenium.

2.3. Preparation of AuNDs/P-rGO-modified electrode

Prior to modification, the GC electrode was thoroughly polished with 0.3 μm and 0.05 μm aqueous slurries of alumina powder, and then sonicated for 3 min in ethanol and water successively. As previously reported [34], the same method was adopted to prepare the nanocomposite material. AuNDs/P-rGO-modified electrodes were synthesized via one-pot electrochemical deposition, and then PB was self-sacrificed by acid-base interaction.

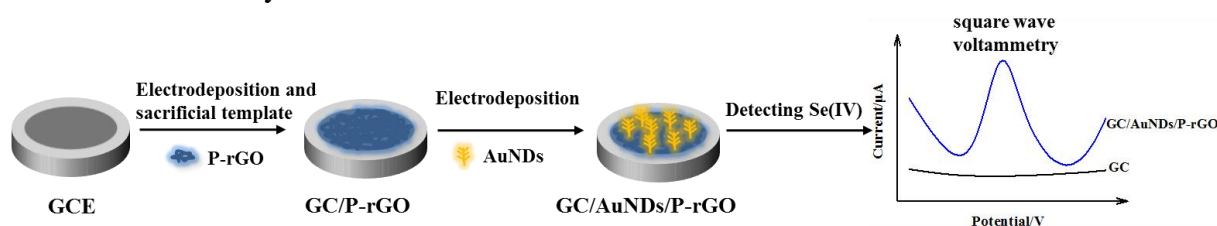


Figure 1. Schematic illustration of the stepwise assembly procedure.

Finally, dendritic gold nanoparticles were electrodeposited. The detailed steps, illustrated in Fig. 1, were as follows: (1) the GC electrode was immersed in a 30 mM aqueous solution containing $K_3Fe(CN)_6$, 30 mM $FeSO_4$, and 0.5 mg/mL GO to electrodeposit rGO@PB films using cyclic voltammetry with a potential range from -1.6 and 1.0 V at a scan rate of 0.2 V s^{-1} for 50 cycles; (2) the rGO@PB-modified electrode was thoroughly rinsed with ultrapure water; (3) the electrode was successively treated with 0.5 M NaOH and 0.1 M H_2SO_4 solutions for five minutes to remove the PB analogues; (4) the AuNDs/P-rGO electrode was prepared by immersing the electrode in 1.0 mM chloroauric acid with added 0.2 M sodium sulfate solution to electrochemically electrodeposit Au nanodendrites with a constant potential of -0.2 V for 20 s; and (5) the obtained GC/AuNDs/P-rGO was washed carefully with deionized water and then dried at room temperature. The perforated graphene oxide (P-rGO) were synthesized by step 1 to 3. For comparison, rGO and AuNDs/rGO-coated GCE were prepared using the same process.

2.4. Electrochemical analysis procedure

Unless stated otherwise, the experiments were carried out in 1 M perchloric acid. Square wave voltammetry (SWV) was scanned over a potential ranging from 0.6 V to 1.2 V using an amplitude of 0.025 V and an equilibrium time of 2 s.

2.5. Preparation of seawater samples

Seawater samples were collected from the Sishi Bay (Yellow Sea, Shandong Province, China) and pretreated as follows: samples were filtered through $0.45\ \mu\text{m}$ membrane filters in acid-cleaned polyethylene bottles and stored at $4\ ^\circ\text{C}$ until analysis. Then, the samples were acidified with certain amounts of HNO_3 and H_2O_2 to obtain a pH less than 2.0. Then, the pre-treated seawater sample was stored at $4\ ^\circ\text{C}$ until analysis. This procedure was used to prevent interactions between samples and microorganisms, and reduce precipitation and complex interactions between targets and other matrix materials. Standard artificial seawater was acidified to obtain a pH less than 2.0 and used for Se(IV) determination.

3. RESULTS AND DISCUSSION

3.1. Morphology of AuNDs/P-rGO-modified electrode

The compositions of the AuNDs/P-rGO were characterized by SEM. As in Fig. 2a and 2b, the dendrite nanogold is evenly distributed on the electrode surface, showing the dendrite structure. In our previous work [34], high magnification and cross-sectional SEM of GC/P-rGO has proved that porous graphene is perfectly synthesized by sacrificing Prussian blue template.

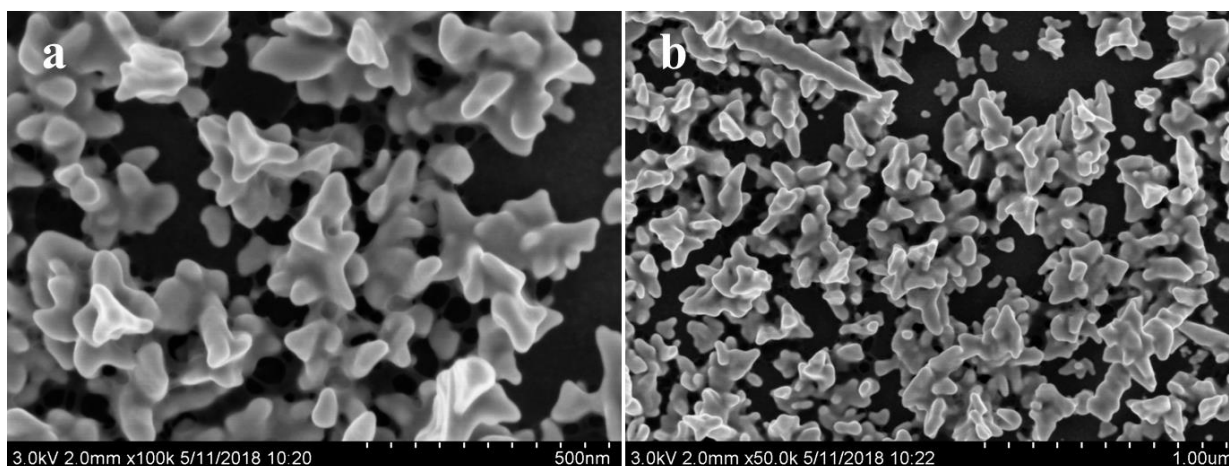


Figure 2. SEM image of GC/P-rGO/AuNDs (a, b)

Prussian blue mentioned on the electrode surface has been completely removed from the electrode surface by alkali washing and pickling, it was characterized by the energy dispersive X-ray spectroscopy (EDS). These results all illustrated that the successful assembly of the AuNDs/P-rGO modified electrode.

3.2. Electrochemical behaviors of AuNDs/P-rGO-modified electrode

GC/AuNDs/P-rGO were analyzed by cyclic voltammetry to evaluate their active surfaces in 5 mM $K_3Fe(CN)_6$ and in $K_4Fe(CN)_6$ containing 0.1 M KCl. According to the slope of I_p on $v^{1/2}$, the active surface area was estimated using the Randles-Sevcik equation [35].

$$I_p = 2.69 \times 10^5 n^{3/2} A D^{1/2} v^{1/2} C_0 \dots\dots(1)$$

where I_p represents the anode peak current, n is the number of transferred electrons, A is the electrode surface area, D is the diffusion coefficient, v is the scanning rate, and C_0 is the concentration of potassium ferricyanide.

According to Equation (1), the current value is proportional to the active area of the modified electrode.

As shown in Fig. 3, the AuNDs, P-rGO, and rGO increased the peak current of the redox probes compared with bare GC electrode. Compared with GC/AuNDs/rGO, the GC/AuNDs/P-rGO showed a remarkably enhanced response current. The peak current of the single-electron redox quasi-reversible reaction of $Fe(CN)_6^{3-/4-}$ using the bare GCE was 1.13×10^{-4} A and 2.59×10^{-4} A in GC/AuNDs/P-rGO. The I_p of modified AuNDs/P-rGO was about 2.3 times higher than that of the bare GC electrode, suggesting that AuNDs and P-rGO enhanced the specific surface area of the electrode. Combined, these results show that the three-dimensional porous structure of P-rGO increased the specific surface area and conductivity of the electrode.

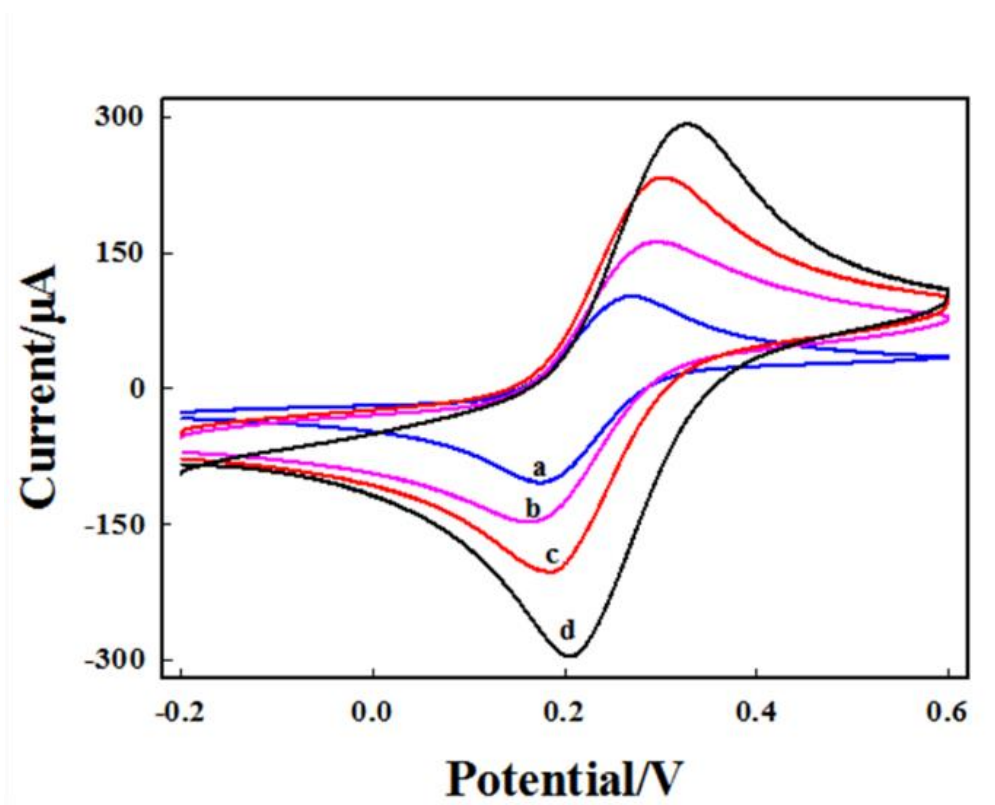


Figure 3. CVs of bare GCE (a), rGO/GCE (b), AuNDs/rGO/GCE (c) and AuNDs/P-rGO/GCE (d) in 5 mM $[\text{Fe}(\text{CN})_6]^{3-/4-}$ solution containing 0.1 M KCl. Scan rate: $100 \text{ mV}\cdot\text{s}^{-1}$.

3.3. Mechanism of Se(IV) determination

The reaction mechanism of Se (IV) may undergo different mechanisms on the electrode in solution, which is rather complicated. However, in acid condition, by applying negative potential, Se (IV) will be reduced to Se element [36,37]. Thus, the electrochemical method can be used to quantify the Se(IV) easily.

3.4. Effect of Se(IV) accumulation potential

The effect of the accumulation potential on the anode peak current at a Se(IV) concentration of 100 nM was investigated when the Se(IV) accumulation time was 180 s and the AuNDs deposition time was 30 s. As shown in Fig. 4a, when the accumulation potential shifted from -0.6 V to -0.5 V, the stripping peak of the current increased, but the stripping current decreased when the potential was further increased from -0.5 V to 0 V. A maximum current was obtained at an accumulation potential of -0.5 V with stirring, therefore, -0.5 V was selected as the optimal accumulation potential.

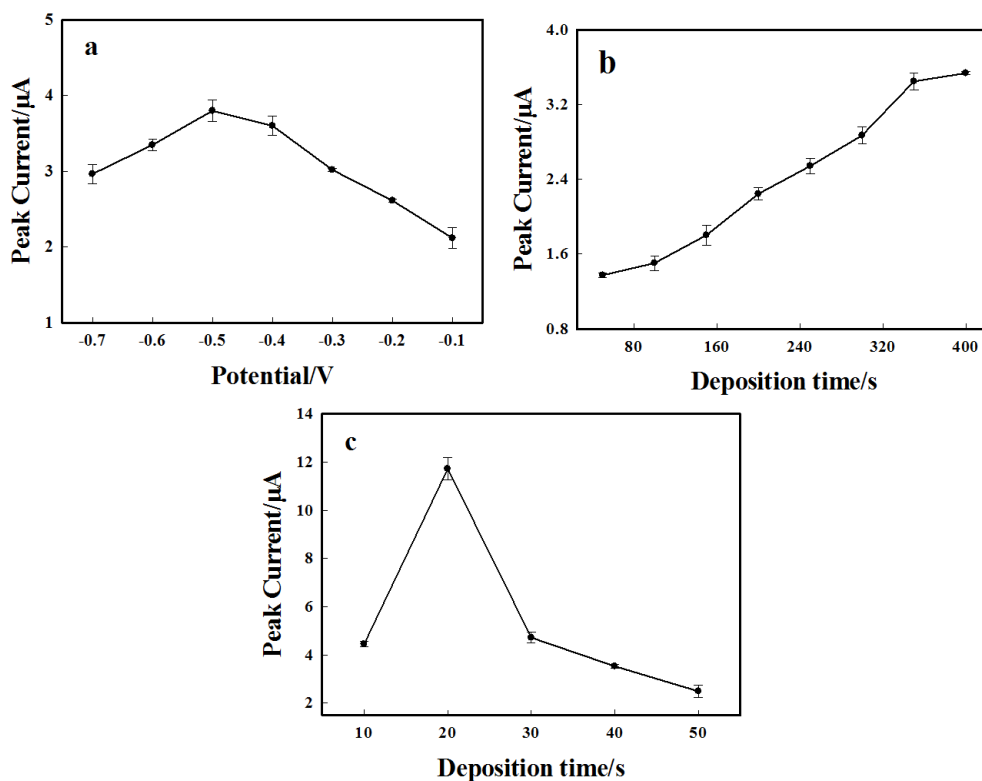


Figure 4. Effect of the Se(IV) accumulation potential (a); Se(IV) accumulation time (b); the gold deposition time (c) in 1 M HClO₄ on AuNDs/P-rGO modified electrode (n=3).

3.5. Effect of Se(IV) accumulation time

The electrochemical response of selenium on the GC/AuNDs/P-rGO surface was studied by setting the accumulation potential to -0.5 V at times ranging from 30 s to 360 s and gold deposition time of 20 s in a solution containing 100 nM Se(IV) (Fig. 4b). The anodic peak current increased linearly with the Se(IV) accumulation time from 30 s to 350 s, but when the time exceeded 350 s, the peak current slowly increased. Considering the analysis time and efficiency, 350 s was selected as the optimal accumulation time.

3.6. Effect of gold deposition time

To obtain the optimal amount of gold deposition, the electrochemical response of Se(IV) on the GC/AuNDs/P-rGO electrode was studied in 1 M HClO₄ solution containing 200 nM Se(IV). The Se(IV) accumulation time and potential were 180 s and -0.5 V, respectively. As shown in Fig. 4c, the gold deposition time ranged from 10 s to 20 s, and the peak anode current gradually increased. However, when the deposition time further increased from 20 s to 50 s, the peak current decreased. This occurred because the AuNDs became larger as the deposition time increased, which masked the function of P-rGO and reduced the specific active surface area of the modified electrode. Therefore, 20 s was selected as the optimum deposition time for AuNDs.

3.7. Calibration curve and detection limit

The calibration curve of Se(IV) in 1 M HClO₄ was obtained using the optimal experimental conditions: a gold deposition time of 20 s, an accumulation potential of -0.5 V, and an accumulation time of 350 s.

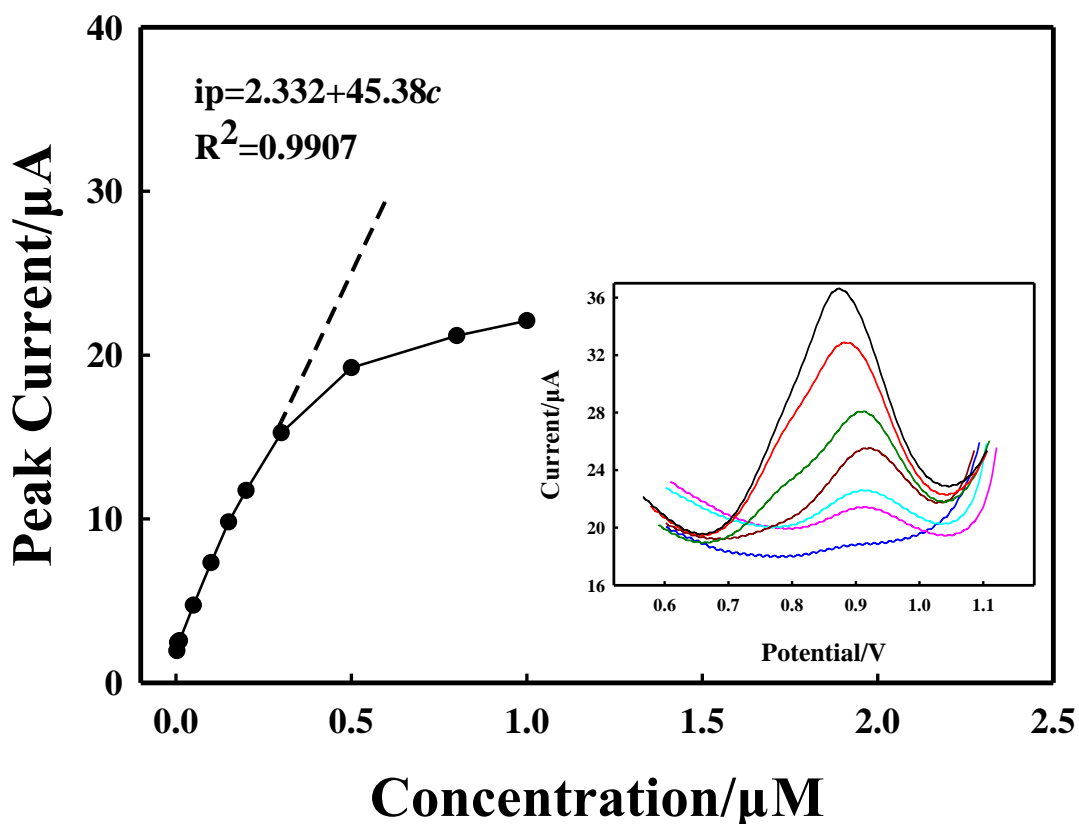


Figure 5. The corresponding calibration curve for selenium determination. Right: SWVs of the AuNDs/P-rGO at different selenium concentrations (from 3 nM to 300 nM) in 1 M HClO₄. Scan rate: 50 mV·s⁻¹.

As shown in Fig. 5, the Se(IV) concentration showed a good linear relationship between 3 nM to 300 nM, and the linear equation was:

$$i_p = 2.332 + 45.38c \quad (2)$$

where, i_p represents the absolute value of peak current, c is the concentration of Se(IV), and the detection limit is 0.9 nM.

Moreover, as shown in Table 1, the AuNDs/P-rGO-modified electrode showed a lower detection limit and higher sensitivity compared with other electrodes.

Table 1. Comparison of analytical methods for Se(IV) determination.

Method	Electrode/agent	Linear range (nM)	Detection limit (nM)	Water sample	Reference
ET-AAS	APDC ^a	0.6-443000	0.06	Fresh water	[22]
HPLC-ICP-MS	RTILs ^b	130-127000	20	Se-rich water	[38]
ED-XRF	GO/CeO ₂	0.9-2.2	200	Underground water	[39]
MP-AES	NaBH ₄	-	126000	Mineral water	[26]
DPCSV ^c	RAgABE ^d	1.9	13-130	Surface water	[16]
DPASV	P-SPE	130-1300	60	Seawater	[24]
SWASV	AuNPs	120-630	2	Seawater	[15]
SWASV	rGO	11	127-633200	Real water	[40]
SWASV	MF-Au ^e	1270-6330	5.3	Stock metal water	[41]
SWASV	AuNDs/P-rGO	3-300	0.9	Seawater	This study

Note: a: Ammonium pyrrolidinedithioate; b: Room temperature ionic liquid; c: Cathodic stripping voltammetry; d: Renewable silver annular band working electrode; e: Micro fabricated gold

3.8. Interferences study

In this work, the electrochemical stripping voltammetry response signal of Se(IV) samples in the presence of interfering ions was tested by adding several possible interfering metals under the optimal operating conditions in a solution containing 50 nM Se(IV). Sb³⁺, Cu²⁺, Fe³⁺, Pb²⁺, Mg²⁺, and Co²⁺ were added in a 100-fold excess versus Se(IV), while a 50-fold excess of Fe³⁺ was used. The results showed that none of these ions significantly interfered with the determination of Se(IV). The obtained results indicated that the GC/AuNDs/P-rGO electrode can be used in the on-line monitor of Se(IV) in real seawater environments.

3.9. Analytical applications

To investigate the practical application of AuNDs/P-rGO-modified electrodes, real seawater samples and artificial seawater with different salinities were analyzed. The standard addition method was used for quantitative analysis, and the accuracy of the method was verified by calculating the recovery rate (%). Due to the low content of Se(IV) in seawater, 20 nM Se(IV) was added to the real

seawater samples for ICP-MS detection. The obtained results using the proposed method and ICP-MS were compared for the determination of Se(IV) in real seawater, as shown in Table 2. The data confirmed that the proposed method for Se(IV) detection is accurate, reliable, and suitable for analyzing Se(IV) in seawater. Moreover, the standard artificial seawater samples with salinities of 4.998 and 34.999 were also tested. The recoveries of standard artificial seawater samples with different salinities (4.998 and 34.999) are shown in Table 2.

Table 2. Results of seawater samples detected by AuNDs/P-rGO modified electrode and ICP-MS.

Sample	Se added (nM)	Proposed method	Recovery (%)	ICP-MS
Seawater sample 1 ^a	0	7.32±0.32	-	-
	20	28.05±0.94	103	27.64±0.49
Seawater sample 2	0	5.03±1.02	-	-
	20	24.37±0.80	97	25.82±1.03
Seawater sample 3	0	6.68±0.43	-	-
	20	28.02±0.56	105	27.15±1.05
Standard artificial seawater samples 1 ^b	0	-	-	-
	20	20.6±0.35	103	-
Standard artificial seawater samples 2 ^c	0	-	-	-
	20	23.6±1.26	118	-

Note:

a: The salinity of the seawater sample 1-3 were all 27.8

b: The salinity of the standard artificial seawater sample 1 was 4.998

c: The salinity of the standard artificial seawater sample 2 was 39.999

The results indicated that the prepared modified electrode exhibited sufficient seawater detection. Moreover, due to its portability and simple operation, prepared modified electrode has many advantages for the on-line determination of Se(IV) in natural seawater environments.

4. CONCLUSIONS

In this work, a AuNDs/P-rGO-modified electrode was successfully and effectively applied to determine Se(IV) in seawater samples and standard artificial seawater samples with different salinities. The proposed method advantages of facile fabrication, a fast analysis speed, high sensitivity and simple pretreatment process exhibit great potential in detecting Se(IV). The obtained results showed that the AuNDs/P-rGO-modified electrode exhibited a higher performance with a lower detection limit, and good accuracy for the detection of Se(IV) in seawater. This method based on GC/AuNDs/P-rGO will be of great benefit for selenium analyses in seawater.

CONFLICTS OF INTEREST

There are no conflicts to declare.

ACKNOWLEDGEMENTS

This work was financially supported by STS Project of Chinese Academy of Science (KFJ-STZ-ZDTP-023), the Key Research and Development Plan of Shandong Province (2017GHY215002), the Senior User Project of RV KEXUE (KEXUE2018G04) and the Key Research and Development Plan of Yantai City (2017ZH096).

References

1. L. Duan, J. Song, X. Li, H. Yuan and S. Xu, *Marine Chemistry*, 121 (2010) 87.
2. H. Dai, S. Wei, L. Skuza and G. Jia, *Ecotoxicology and Environmental Safety*, 180 (2019) 179.
3. Q. Zhang, W. Li, J. Wang, B. Hu, H. Yun, R. Guo and L. Wang, *Biological trace element research*, 191 (2019) 354.
4. P. Kumkrong, K. L. LeBlanc, P. H. J. Mercier and Z. Mester, *Science of the Total Environment*, 640 (2018) 1611.
5. K. L. LeBlanc, P. Kumkrong, P. H. J. Mercier and Z. Mester, *Science of the Total Environment*, 640 (2018) 1635.
6. V. S. Saji and C.-W. Lee, *Rsc Advances*, 3 (2013) 10058
7. S. Ulusoy, S. Mol, F. S. Karakulak and A. E. Kahraman, *Biological Trace Element Research*, 191 (2019) 207.
8. J. E. Conde and M. S. Alaejos, *Chemical Reviews*, 97 (1997) 1979.
9. X. P. Yu, M. X. Wang, X. J. Nan, Y. F. Guo and T. L. Deng, *Water Environment Research*, 91 (2019) 292.
10. S. J. Fairweather-Tait, Y. P. Bao, M. R. Broadley, R. Collings, D. Ford, J. E. Hesketh and R. Hurst, *Antioxidants. Redox Signaling*, 14 (2011) 1337.
11. C. Wang, M. He, B. Chen and B. Hu, *Talanta*, 188 (2018) 736.
12. C. K. Su and W. C. Chen, *Microchimica Acta*, 2018, 185.
13. C. Plessl, B. M. Gilbert, M. F. Sigmund, S. Theiner, A. Avenant-Oldewage, B. K. Keppler and F. Jirsa, *Science of the Total Environment*, 659 (2019) 1158.
14. H. J. Sun, B. Rathinasabapathi, B. Wu, J. Luo, L.-P. Pu and L. Q. Ma, *Environment International*, 69 (2014) 148.
15. R. Segura, J. Pizarro, K. Diaz, A. Placencio, F. Godoy, E. Pino and F. Recio, *Sensors and Actuators B-Chemical*, 220 (2015) 263.
16. B. Bas, K. Jedlinska and K. Wegiel, *Electrochemistry Communications*, 49 (2014) 79.
17. H. Wei, D. Pan, X. Hu, M. Liu, H. Han and D. Shen, *Microchimica Acta*, 185 (2018) 285.
18. W. Wu, Z. Y. Liu, X. G. Li and C. W. Du, *Journal of Electroanalytical Chemistry*, 845 (2019) 92.
19. J. Miao, Z. L. Lang, X. Y. Zhang, W. G. Kong, O. W. Peng, Y. Yang, S. P. Wang, J. J. Cheng, T. C. He, A. Amini, Q. Y. Wu, Z. P. Zheng, Z. K. Tang and C. Cheng, *Advanced Functional Materials*, 29 (2019) 9.
20. N. Campillo, R. Penalver, I. Lopez-Garcia and M. Hernandez-Cordoba, *Journal of Chromatography A*, 1216 (2009) 6735.
21. X. Peng and Z. Wang, *Analytical chemistry*, 91 (2019) 10073.
22. E. Ghasemi, N. M. Najafi, F. Raofie and A. Ghassempour, *Journal of Hazardous Materials*, 181 (2010) 491.
23. C. Wang, M. He, B. Chen and B. Hu, *Talanta*, 188 (2018) 736.
24. A. V. Kolliopoulos, J. P. Metters and C. E. Banks, *Analytical Methods*, 5 (2013) 851.
25. A. O. Idris, N. Mabuba and O. A. Arotiba, *International Journal of Electrochemical Science*, 12

- (2017) 10.
26. I. V. Mikheev, E. A. Karpukhina, L. O. Usoltseva, T. O. Samarina, D. S. Volkov and M. A. Proskurnin, *Inorganic Materials*, 53 (2017) 1422.
 27. S. Y. S. Jaber, A. Ghaffarinejad and E. Omidinia, *Analytica Chimica Acta*, 1078 (2019) 42.
 28. Q. A. Drmash, A. H. Hendi, M. K. Hossain, Z. H. Yamani, R. A. Moqbel, A. Hezam and M. Gondal, *Sensors and Actuators B-Chemical*, 290 (2019) 666.
 29. X. Gao, Y. Gao, C. Bian, H. Ma and H. Liu, *Electrochimica Acta*, 310 (2019) 78.
 30. S. Kokarnig, A. Tsirigotaki, T. Wiesenhofer, V. Lackner, K. A. Francesconi, S. A. Pergantis and D. Kuehnelt, *Journal of Trace Elements in Medicine and Biology*, 29 (2015) 83.
 31. T. Wang, Y. Fu, L. Bu, C. Qin, Y. Meng, C. Chen, M. Ma, Q. Xie and S. Yao, *Journal of Physical Chemistry C*, 116 (2012) 20908.
 32. H. L. B. Bostrom and R. I. Smith, *Chemical communications*, 55 (2019) 10230.
 33. Y. Wang, S. Chen and J. Zhang, *Advanced Functional Materials*, 29 (2019) 45.
 34. H. Wei, D. Pan, S. Ma, G. Gao, D. Shen, *Analytist*, 144 (2019) 412.
 35. K. Jayakumar, M. B. Camarada, R. Rajesh, R. Venkatesan, H. X. Ju, V. Dharuman, Y. P. Wen, *Biosensors and Bioelectronics*, 120 (2018) 55.
 36. V. Beni, G. Collins, D. W. Arrigan, *Analytica Chimica Acta*, 699 (2011) 127.
 37. A. Manzoli, M.C. Santos, S.A.S. Machado, *Thin Solid Films*, 515 (2007) 6860.
 38. B. Chen, M. He, X. Mao, R. Cui, D. Pang and B. Hu, *Talanta*, 83 (2011) 724.
 39. A. Baranik, R. Sitko, A. Gagor, I. Queralt, E. Margui and B. Zawisza, *Analytical Chemistry*, 90 (2018) 4150.
 40. A. O. Idris, N. Mabuba, D. Nkosi, N. Maxakato and O. A. Arotiba, *International Journal of Environmental Analytical Chemistry*, 97 (2017) 534.
 41. S. H. Tan and S. P. Kounaves, *Electroanalysis*, 10 (1998) 364.